WRDC-TR-90-2070

TRANSIENT HYDROGEN HEAT TRANSFER

Beverly Louie
National Institute of Standards and Technology
325 Broadway
Boulder, CO 80303-3328

W. Gene Steward
FluidTherm Engineering
Sugarloaf Road
Boulder, CO 80302

August 1, 1990

Final Report for Period April 1986 - April 1989

AERO PROPULSION AND POWER LABORATORY
WRIGHT RESEARCH DEVELOPMENT CENTER
AIR FORCE SYSTEMS COMMAND
WRIGHT-PATTERSON AIR FORCE BASE, OHIO 45433-6563

NOTICE

WHEN GOVERNMENT DRAWINGS, SPECIFICATIONS, OR OTHER DATA ARE USED FOR ANY PURPOSE OTHER THAN IN CONNECTION WITH A DEFINITELY GOVERNMENT-RELATED PROCUREMENT, THE UNITED STATES GOVERNMENT INCURS NO RESPONSIBILITY OR ANY OBLIGATION WHATSOEVER. THE FACT THAT THE GOVERNMENT MAY HAVE FORMULATED OR IN ANY WAY SUPPLIED THE SAID DRAWINGS, SPECIFICATIONS, OR OTHER DATA, IS NOT TO BE REGARDED BY IMPLICATION, OR OTHERWISE IN ANY MANNER CONSTRUED, AS LICENSING THE HOLDER, OR ANY OTHER PERSON OR CORPORATION; OR AS CONVEYING ANY RIGHTS OR PERMISSION TO MANUFACTURE, USE, OR SELL ANY PATENTED INVENTION THAT MAY IN ANY WAY BE RELATED THERETO.

THIS TECHNICAL REPORT HAS BEEN REVIEWED AND IS APPROVED FOR PUBLICATION.

CHARLES E. OBERLY, Project Engineer
Applied Electromagnetics Section
Advanced Power Systems Branch

STEPHEN D. VINING, Lt Col, USAF
Atg Chf, Advanced Pwr Systems Branch
Aerospace Power Division

FOR THE COMMANDER

MICHAEL D. BRAYDICH, Lt Col, USAF
Deputy Director
Aerospace Power Division
Aero Propulsion and Power Directorate

IF YOUR ADDRESS HAS CHANGED, IF YOU WISH TO BE REMOVED FROM OUR MAILING LIST, OR IF THE ADDRESSEE IS NO LONGER EMPLOYED BY YOUR ORGANIZATION PLEASE NOTIFY WL/POOX-2, WRIGHT-PATTERSON AFB, OH 45433-7919 TO HELP MAINTAIN A CURRENT MAILING LIST.

COPIES OF THIS REPORT SHOULD NOT BE RETURNED UNLESS RETURN IS REQUIRED BY SECURITY CONSIDERATIONS, CONTRACTUAL OBLIGATIONS, OR NOTICE ON A SPECIFIC DOCUMENT.

REPORT DOCUMENTATION PAGE

Form Approved
OMB No. 0704-0188

1. AGENCY USE ONLY (Leave blank)	2. REPORT DATE	3. REPORT TYPE AND DATES COVERED
	1 August 1990	Final Technical Report April 1986-1989

4. TITLE AND SUBTITLE

Transient Hydrogen Heat Transfer

5. FUNDING NUMBERS

MIPR-FY1455-89-N0606

6. AUTHOR(S)

B. Louie and W. G. Steward

7. PERFORMING ORGANIZATION NAME(S) AND ADDRESS(ES)

National Institute for Standards and Technology
325 Broadway
Boulder CO 80303-3325

8. PERFORMING ORGANIZATION REPORT NUMBER

---

9. SPONSORING/MONITORING AGENCY NAME(S) AND ADDRESS(ES)

Wright Laboratory
WL/POOX-2 Bldg 450
2645 Fifth St Ste 13
Wright-Patterson AFB OH 45433-7919

10. SPONSORING/MONITORING AGENCY REPORT NUMBER

WRDC-TR-90-2070

11. SUPPLEMENTARY NOTES

12a. DISTRIBUTION/AVAILABILITY STATEMENT

Unlimited

12b. DISTRIBUTION CODE

13. ABSTRACT *(Maximum 200 words)*

The Chemical Engineering Science Division (Boulder CO) of the National Institute of Standards and Technology has investigated transient heat transfer to liquid hydrogen. Thin carbon films and Pt foils submerged in liquid hydrogen received stepped inputs of power of 1 to 42 W/cm^2, and the onset of nucleate or film boiling was obtained for each power level. The critical heat flux was found to be approximately 8 W/cm^2, with the transition to film boiling occurring in times less than 10^{-3} S. Premature film boiling can be related to the positive temperature coefficient of resistance and the narrowness of the heaters. Thermometric devices and power generation equipment selection are discussed.

14. SUBJECT TERMS

Liquid Hydrogen Heat Transfer
Nucleate Boiling Onset

15. NUMBER OF PAGES

40

16. PRICE CODE

17. SECURITY CLASSIFICATION OF REPORT	18. SECURITY CLASSIFICATION OF THIS PAGE	19. SECURITY CLASSIFICATION OF ABSTRACT	20. LIMITATION OF ABSTRACT
UNCLASSIFIED	UNCLASSIFIED	UNCLASSIFIED	UL

CONTENTS

LIST OF FIGURES

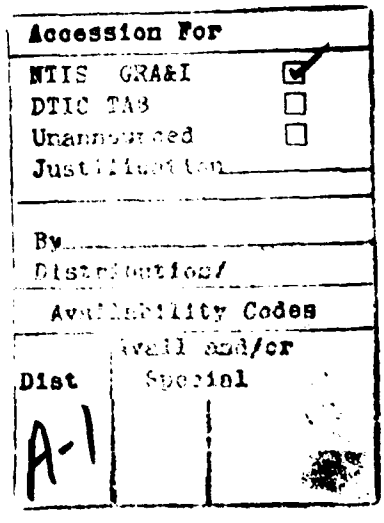

Transient Hydrogen Heat Transfer*
Final Report for April 1986 – April 1989

B. Louie
Chemical Engineering Science Division
National Institute of Standards and Technology
Boulder, Colorado 80303–3328

W. G. Steward
FluidTherm Engineering
Boulder, Colorado 80302

We have investigated transient heat transfer to liquid hydrogen. Thin carbon films and Pt foils submerged in liquid hydrogen received stepped inputs of power ranging from 1 to 42 W/cm^2, and the onset of nucleate or film boiling was obtained for each power level. The critical heat flux was found to be approximately 8 W/cm^2, with the transition to film boiling occurring in times less than 10^{-3} s. Premature film boiling can be related to the positive temperature coefficient of resistance and the narrowness of the heaters. Thermometric devices and power generation equipment selection are discussed.

1. INTRODUCTION

The goal of this study is to fill the void in data for transient heat transfer in liquid hydrogen. The experimental technique has been previously used in liquid helium [1,2,3] and liquid nitrogen, [1,4,5] and uses stepped inputs of power to submerged heaters. The duration of the input ranges from 10^{-5} to 10 s, with the onset of nucleate boiling occurring in times on the order of 10^{-3} s. The surface temperature is monitored throughout the period of application of power.

In Section 2 the report describes the selection and assembly of the experimental apparatus, including the safety considerations for using liquid hydrogen at NIST, and the various heater/thermometers used. An analysis of transient heat transfer behavior is presented in Section 3, followed by a presentation of experimental results in Section 4. Finally, the conclusions are given in Section 5.

Keywords: boiling; conduction; hydrogen; premature film boiling; thermometry; transient heat transfer

---

*Publication of the National Institute of Standards and Technology, not subject to copyright.
Work performed under WPAFB MIPR contract number FY1455–89–N0604.

2. EXPERIMENTAL APPARATUS AND PROCEDURE

Procedures used in these experiments were subject to the NIST guidelines for the laboratory use of liquid hydrogen [6]. The prevention of backflow of air into the apparatus, dewar breakage, and the normal venting from the experiment were specifically identified as safety concerns. Because this study focused on transient behavior, many potential hazards were minimized by the size of the experiment. Less than 2 liters of liquid hydrogen were used in any one experiment, and the duration of an experiment was less than half a day. Also, experiments in liquid nitrogen enabled us to identify potentially hazardous techniques which were then modified for use with liquid hydrogen.

The experimental technique used for this study was the application of a step in power applied to a thin film resistance device. The change in resistance of this device was used to determine the temperature change and heat transfer characteristics at the its surface and . The selection of the appropriate electronic equipment and test devices is summarized in this section.

2.1 Overview of the Experimental Apparatus

A small, vacuum–jacketed dewar with optical viewports was used as the cryostat. Liquid nitrogen shielded the dewar. The test section was mounted vertically at the end of a long rod in the neck of the dewar. The temperature of the bath was measured with a germanium resistance thermometer. The assembly is shown in Figure 1. The dewar was surrounded with a plexiglass shield and metal curb, which served as protection from glass fragments from dewar breakage. O–ring seals were used on the flange fitting for the main dewar compartment and for the electrical leads.

During an experiment the vent gas left the dewar and was warmed to ambient temperature within a large copper coil, passed through two check valves, and exited above the rooftop. The check valves prevented backflow of air into the apparatus. An electrochemical hydrogen detector was located above the dewar. The instrument rack was purged with fresh air during experiments.

2.2 Power Generation Devices

An ideal step or pulse input of power has a very short rise time with a minimal overshoot, a period of steady power, and a fast shutoff with a minimal backswing. Most power supplies are designed for a specific resistive load in order to produce the ideal waveform. Changing the size of the resistive load can significantly distort the shape of the power input. Consider, too, that limitations in the range of a power supply can dictate what the resistance of the load must be. Finding acceptable solutions to this trial–and–error problem is most important in obtaining useful data. Several power generators were used in this study to attempt to match impedances with the various test sections. Following is a summary of the various power supplies used.

Square wave pulse generator. This pulse generator was built by the Fracture and Deformation Division of NIST. It had a pulse width of either 10^{-6} or 10^{-5} s, a maximum current of 20 A and voltage output of 50 V, and was designed to handle a resistive load of 2.5 to 2.6 ohms. This unit was limited to the production of repetitive pulses which were unfortunately characterized by large negative backswings; hence, it was used only to obtain preliminary data.

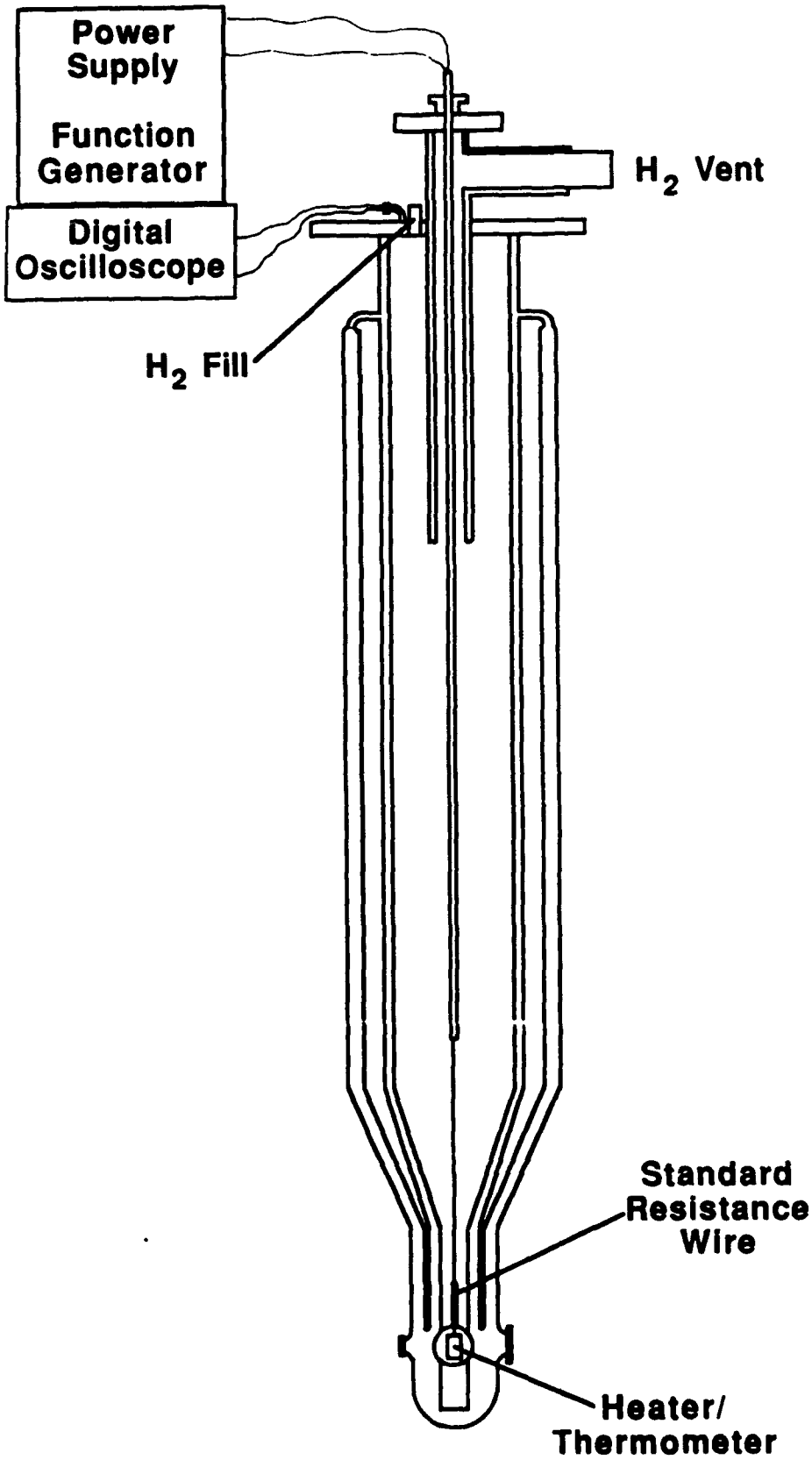

Figure 1. Schematic of experimental apparatus.

High power pulse generator. This commercially available generator could produced either single or repetitive pulses (up to 30 kHz) and variable pulse widths (approximately 10^{-6} to 10^{-3} s), by using different plug-in modules to set the output. The voltage ranged from 48 to 1000 V and the current, from 5 to 100 A, depending on the module. The pulses produced by this apparatus exhibited an overshoot of up to 15% and negative backswing, but both characteristics were modulated by proper choice of load impedance and by the addition of several electrical components on the output. The electrical circuit is shown in Figure 2. The largest drawback of this unit was the duration of the pulse. It was found that constant power could not be maintained for longer than 10^{-3} s, which is the minimum time required to reach steady-state boiling in either liquid nitrogen or liquid hydrogen. Also, some of the output units exhibited a ramping output power atypical of specifications. This unit was limited for use only in producing short, high power pulses.

Square-wave pulse generator with built-in delay. We also used on a limited basis a third pulse generator fabricated in our Division for other transient heat transfer experiments. This unit has a single 1 to 100 A square pulse of 10^{-3}s to 1 s duration. This generator is incapable of producing pulses shorter than 10^{-3} s or less than 1 A in amplitude. Since it was an integral component of another experiment, its availability was restricted.

Bipolar power amplifier with function generator. A bipolar power amplifier with a function generator was used to provide step inputs of low to medium power. Its maximum voltage is 72 V. Power inputs of 0.01 to 55 W/cm^2 were used. This unit has a maximum current output of 5 A, which was found to be insufficient for some tests. Since it can operate in a fast mode, with ramp times of less than 2.5×10^{-5} s, it was able to produce clean, square, stepped input of power.

2.3 Transient Response Thermometry

The selection of thin film resistance devices for transient response thermometry was guided by several factors. It is desirable to select a material which has a fast response as a heater and whose resistance is a known function of temperature. A single device used as both the heater and thermometer would eliminate the temperature difference and time lags in heat transfer between the heater and thermometer. Platinum was identified as a potential material because of its suitable resistance response in the 20 K range and its ease of fabrication into usable devices. Carbon films demonstrated characteristics which proved beneficial to obtaining fast temperature responses. For all devices used, significant study was required to match the impedance of the heater/thermometer with that of the power generator, while optimizing the heat transfer geometry. This section will discuss our experience with each type of heater/thermometer, briefly indicating the suitability of each device.

Vapor-deposited films. Several vapor-deposited, platinum thin film resistance devices on quartz substrates were fabricated to our design by the Cryoelectronics Division at NIST in Boulder to serve as heaters and as thermometers. A schematic of a film is shown in Figure 3. The thickness of the devices ranged from 1 to 4×10^{-5} cm. The resistance was adjusted by increasing path length of the platinum with a serpentine pattern. These test sections exhibited poor sensitivity at low temperatures, with an average resistivity ratio R_{rt}/RR_{273} at 77 K of 0.6. Although annealing the thin films at 550 °C appeared to relieve fabrication stress points, the resistivity ratio at 77 K improved only to 0.45. The resistivity ratios at 20 K and 4 K were both 0.25, indicating no sensitivity at these lower temperatures. This behavior

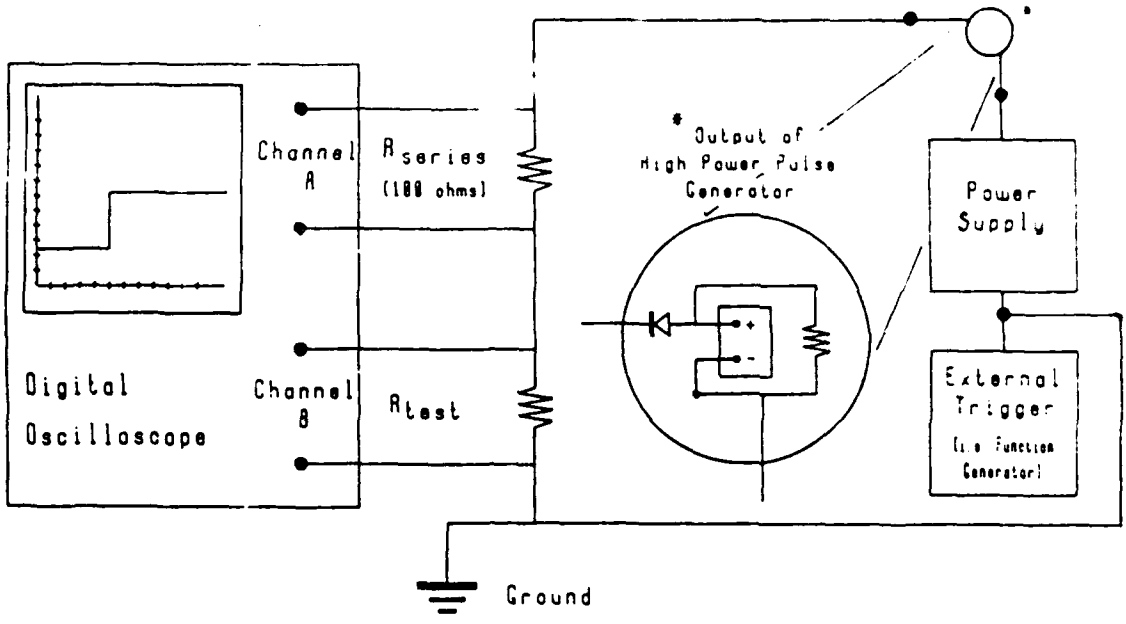

Figure 2. Schematic of electrical circuit for transient hydrogen heat transfer experiments.

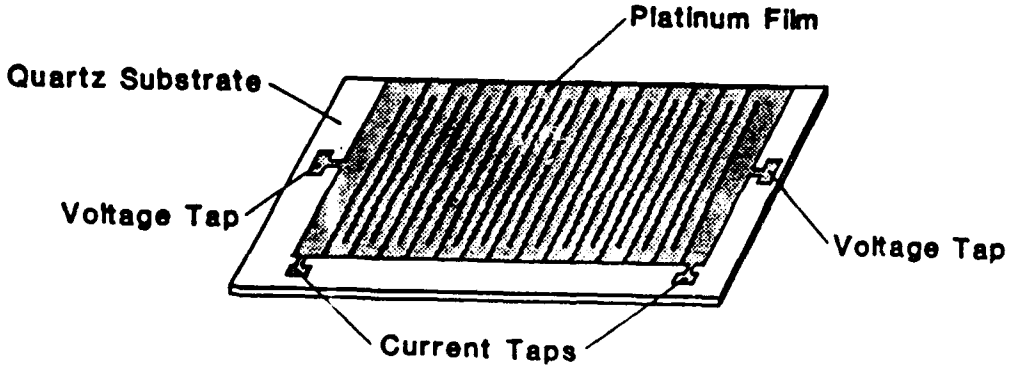

Figure 3. Schematic of vapor-deposited Pt film on a quartz substrate for use as a heater and thermometer.

is similar to that of an impure metal and suggests that the mean free path of the electrons is larger than the thickness of the film. Attempts to increase the thickness of the films failed. Consequently, these heater/thermometers could not be used in these experiments.

Platinum foil on quartz and fiberglass–epoxy substrates. Pieces of platinum foil 4 x 10^{-4} cm thick were mounted on quartz or fiberglass epoxy substrates and cut into serpentine patterns to reach a specific resistance. A schematic drawing of this heater/thermometer is shown in Figure 4. The resistivity ratios at 77 K and 4 K for unsupported samples of foil were RR_{rt}/RR_{273} = 0.185 and 0.0138, respectively. Preliminary data for heat fluxes less than 20 W/cm² in saturated liquid hydrogen showed fast response and high sensitivity.

There were problems with this design. These thermometers had to be "trained" before they would hold a steady resistance at low temperatures. After cycling 20 to 30 times between LN_2 and room temperature, the resistance would stabilize at 77 K and below. We postulate that the difference in the thermal expansion between the substrate and the platinum foil induced stress points in the serpentine structure. Frequently the devices exhibited an open circuit at low temperatures. Another problem was that data for heat fluxes higher than 20 W/cm² were unobtainable, due to current limitations in the power supplies.

Another concern was an unusual temperature response prior to true nucleate boiling, which was not supported by known conduction behavior. We speculated that the response might be attributed to substrate effects, poor convection at the heater surface, or an inelastic interaction between the heater surface and substrate. Additional data now indicates that the pattern of the Pt foil encourages the early transient behavior. A detailed discussion of these results is given later in this report.

Thick film platinum resistance devices on alumina. It was assumed that current limitations would not be encountered when using these small, thick film devices. These commercially manufactured temperature detectors have a meandering pattern of Pt, which appears to be sputtered on the alumina support. The pattern could be partially shunted to change the overall resistance of the device and thereby match the desired impedances. We obtained a resistance of 10 to 12 Ω at 77 K, and the resistivity ratio R_{rt}/RR_{273} was 0.02. During calibration in LN_2 significant self–heating was found. Also, unusually small changes in resistance in response to large power inputs were observed. Calculations confirmed the experimental results and showed that 90% of the heat input was absorbed by the alumina. Several devices were burned out during preliminary testing.

Unsupported platinum foil. Calculations show that a quartz or fiberglass epoxy substrate could absorb up to 30% of the heat input in liquid nitrogen and 10% in liquid hydrogen. These calculations combined with the data indicating the previously described, unusual transient behavior prompted the development of an unsupported platinum foil heater/thermometer. Our experience with the multichannel, supported heater/thermometer indicated that a single ribbon of platinum could be used as the test section. A schematic of this configuration is shown in Figure 5. We used various devices of this type to study premature film boiling as a function of size and heat input. A detailed discussion of the results is provided in Section 4.

Carbon films. Carbon has a negative temperature coefficient of resistance, the opposite of platinum, and a relatively high resistance. These attributes made it

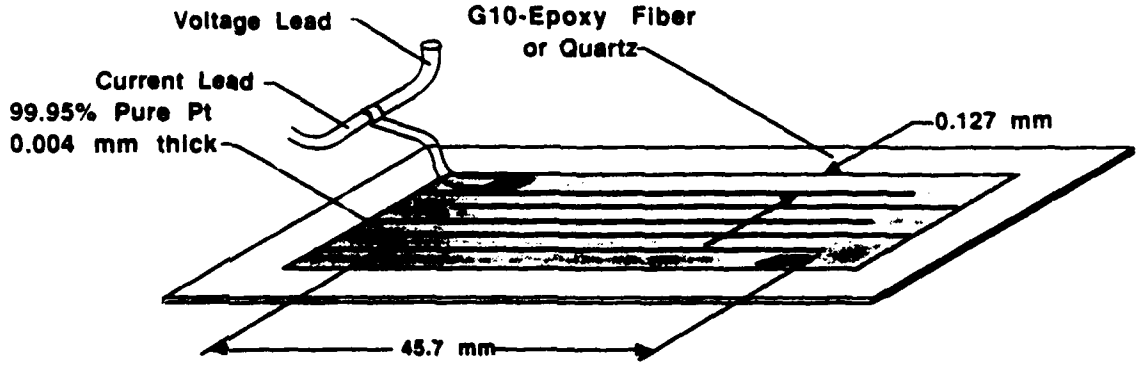

Figure 4. Schematic of Pt foil deposited on quartz substrate for use as a heater/thermometer.

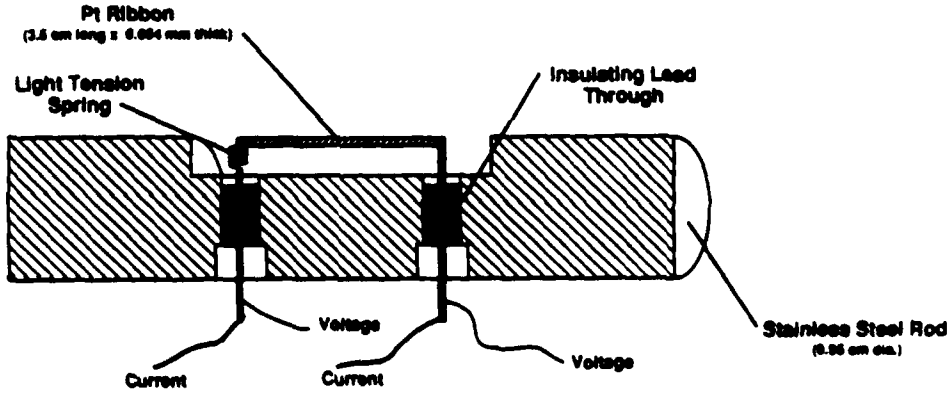

Figure 5. Schematic of unsupported Pt foil heater/thermometer.

difficult to choose a carbon test section for use with the existing electronics. For example, the resistance of an unsupported Pt film at 20 K often was 1 Ω or less, while the carbon film had resistance of nearly 800 Ω. Several benefits were found from using the carbon devices. First, a large voltage could be obtained which could overcome system noise. This meant a voltage response which was up to 800 times larger than that of the unsupported Pt foil was recorded. A second result was the reduction in the current required. The current required was typically 0.1 A or less, a value well below the 5 A limit of the power supply. The limiting factor, therefore, was not the magnitude of the heat input, but whether the carbon device could physically withstand high power.

Several carbon films were tested. The first "film" was a strand of fine carbon fibers stretched across a quartz substrate. Its indefinite heat transfer area made this device of questionable value. The second film was made of pressed graphite powder on quartz. This device showed good sensitivity when calibrated in the temperature range within ±5 K of 77 K. However, the voltage response prematurely leveled out during applications of pulses between 5 and 20 W/cm^2. Based on previous transient LN_2 studies [1] a transition to nucleate boiling occurs at 10^{-2} to 10^{-1} s; by contrast, our results show a steady state voltage occurring as early as 8×10^{-4} s. We surmise that the results are related to the quality of the carbon film. Since the film was made by rubbing graphite onto quartz, the particles are only loosely held together in a film of varying thickness. Perhaps this combination of roughness and agglomeration enables the formation of "channels" which divert the flow of electrons through a path of least resistance, which decreases as more heat is applied.

The third device, shown in Figure 6, is a thin carbon film deposited on quartz by an electron beam. The device has been used in previous heat transfer experiments [7]. Its dimensions are approximately 4.11 mm x 6.35 mm. Preliminary results with this heater/thermometer submerged in LN_2 confirmed earlier results reported by Steward [1], which warranted its use in LH_2.

2.4 Data Acquisition

A two–channel digital oscilloscope was used to record the voltage response of the heater/thermometer and the standard resistance wire from which current was determined. The oscilloscope has ranges of 200 mV to 80 V full scale. A total of 7964 points can be obtained for each channel with 12–bit resolution at 100 ns/point. The voltage responses were displayed on the display screen and recorded on diskette. An 80286–based desktop computer was used for data analysis following each run. Data were transmitted by RS–232 cable by using a commercially available software package.

2.5 Experimental Procedure

The experimental dewar was filled according to the NIST guidelines [6]. The dewar was purged with gaseous nitrogen followed by gaseous hydrogen, prior to filling with liquid hydrogen. Safety procedures included posting warning signs donning conducting ankle straps, and arming the hydrogen leak detection alarms.

Electrical connections were made through an air–tight feedthrough at the top of the dewar. A schematic circuit diagram is shown in Figure 2. The test procedure began by applying a low voltage to the test section until the desired heat flux was verified by a spot computation. The step inputs were initially of 10^{-4} s duration, and incrementally increased up to 10 s. The power was likewise modified in small increments, and each response was recorded.

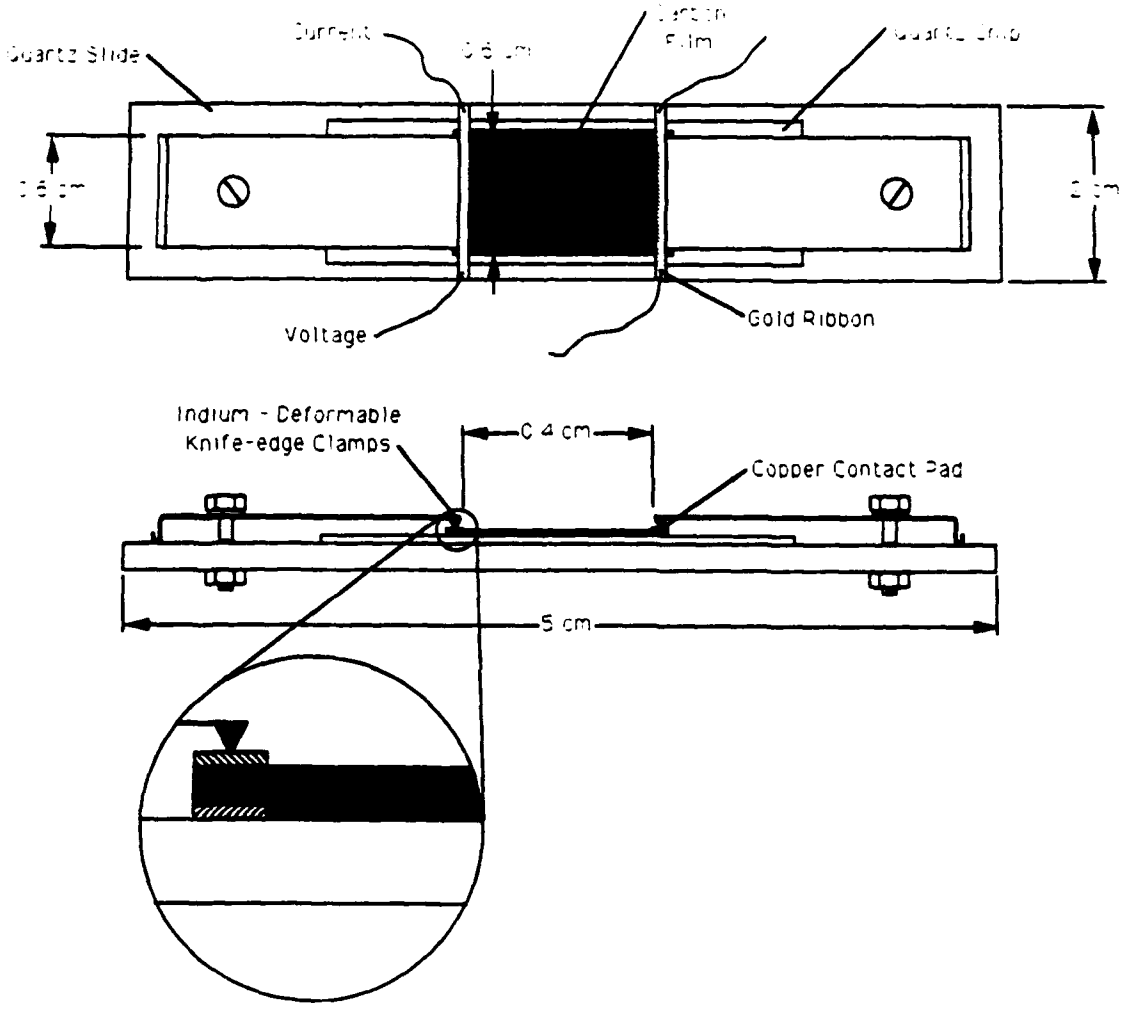

Figure 6. Schematic of carbon thin film deposited on a quartz substrate used as a heater/thermometer

3. ANALYSIS OF TRANSIENT CONDUCTION HEAT TRANSFER

Immediately following a step heat input, until the beginning of natural convection and boiling, the heat transfer from solid to liquid obeys the law of conduction. Comparison of the measured temperatures with conduction calculations is a reliable way of verifying the accuracy of transient temperature measurements, and the point of digression marks the beginning of convection and boiling. The two configurations, (1) thin films of Pt or carbon deposited on a solid substrate, and (2) suspended Pt ribbons without a substrate, require two different solutions of the transient conduction equation.

3.1 Thin Films on Solid Substrates

Vapor–deposited films have so little mass compared to the substrate that the sensible heat of the film, its thickness, and any temperature difference across it may be neglected. The following expression, for which the variables are defined in the Nomenclature section at the end of the paper,

$$T = \frac{2}{\sqrt{\pi}} \frac{Q\sqrt{t}}{\frac{k_s}{\sqrt{\alpha_s}} + \frac{k_f}{\sqrt{\alpha_f}}}, \qquad (1)$$

for the heater surface temperature of a thin film was derived previously [1] and is presented in Appendix A of this report.

3.2 Ribbon Heater/Thermometer *without* a *Substrate*

Free–standing ribbons are thicker than vapor deposited films, and the heat capacity of the solid as well as possible temperature gradients must be accounted for. The two required differential equations are for the deposited film and the liquid, rather than its substrate and the liquid. The following closed–form solution for the temperature may be obtained through use of Laplace transforms:

$$T' = t' - \frac{1}{\beta+1} \sum_{n=1}^{\infty} \left[\frac{\beta-1}{\beta+1}\right]^n \int_0^{t'} \left[\operatorname{erfc}\left[\frac{2n+1}{2\sqrt{\theta}} - z'\right] + \operatorname{erfc}\left[\frac{2n+1}{2\sqrt{\theta}} + z'\right]\right] d\theta \,. \qquad (2)$$

A full derivation is presented in Appendix B.

4. RESULTS AND DISCUSSION

From measurements of voltage across the test section of a heater/thermometer and voltage across a standard resistor in series, the power per unit surface area, Q, is

$$Q = (V_t)(V_s)/(R_s A), \tag{3}$$

and the test section resistance is

$$R_t = (V_t)(R_s)/V_s . \tag{4}$$

The test section temperature T is found from

$$T = T(R_t), \tag{5}$$

where $T(R_t)$ is the calibration function for the particular heater/thermometer.

4.1 Transient Heat Transfer to Liquid Hydrogen Using Carbon Films

Calculations of conduction heat transfer compared to the experimental data carbon films are shown in Figures 7 and 8 for powers from 1.15 to 42 W/cm², with heater temperature rise as a function of time. The data agree with calculations within experimental error except for a slight deviation toward the end of the period, possibly due to early nucleation at preferred sites. The deviation in slope of the data from the conduction calculations indicates that steady nucleate boiling has been reached. At 7.8 W/cm², after a period of steady temperature the data exhibit a small overshoot at 0.05 s. Since the slope of the temperature data returns to the previous level, this change in slope may indicate localized film boiling. The heat flux of 7.8 W/cm² corresponds well to the steady-state Kutateladze prediction [8] of 9 W/cm² for the nucleate boiling maximum or critical heat flux in liquid hydrogen. For heat fluxes of 10.8 W/cm² and higher, sharp transitions into film boiling can be discerned after a period of metastable nucleate boiling, shown by a gradual increase in temperature.

4.2 Premature Film Boiling Using Pt Foil Heater/Thermometers

Heater/thermometers of supported and unsupported Pt foil were used to study premature film boiling in LH_2. Premature film boiling, distinguished by a sudden, unexpected transition to film boiling, has been noted for LN_2 and LH_2 in transient stepped power tests with thin Pt films.[4,5] We never observed this behavior with the carbon film.

An estimate for the time, t_f, when a transition to film boiling takes place at a solid–liquid interface can provides a basis for evaluating premature film boiling. Schmidt [2] developed a correlation for LHe for t_f, which is given by

$$t_f = \gamma^2 \left[\frac{k}{\rho c}\right]\left[\frac{L}{Q}\right]^2 . \tag{6}$$

Equation (6) is plotted on Figure 9 and has a slope proportional to Q^{-2}; γ is computed from carbon film experimental data and fluid properties for LH_2. We modified Equation (6) to reflect the fact that t_f approaches infinity at the critical heat flux, and to

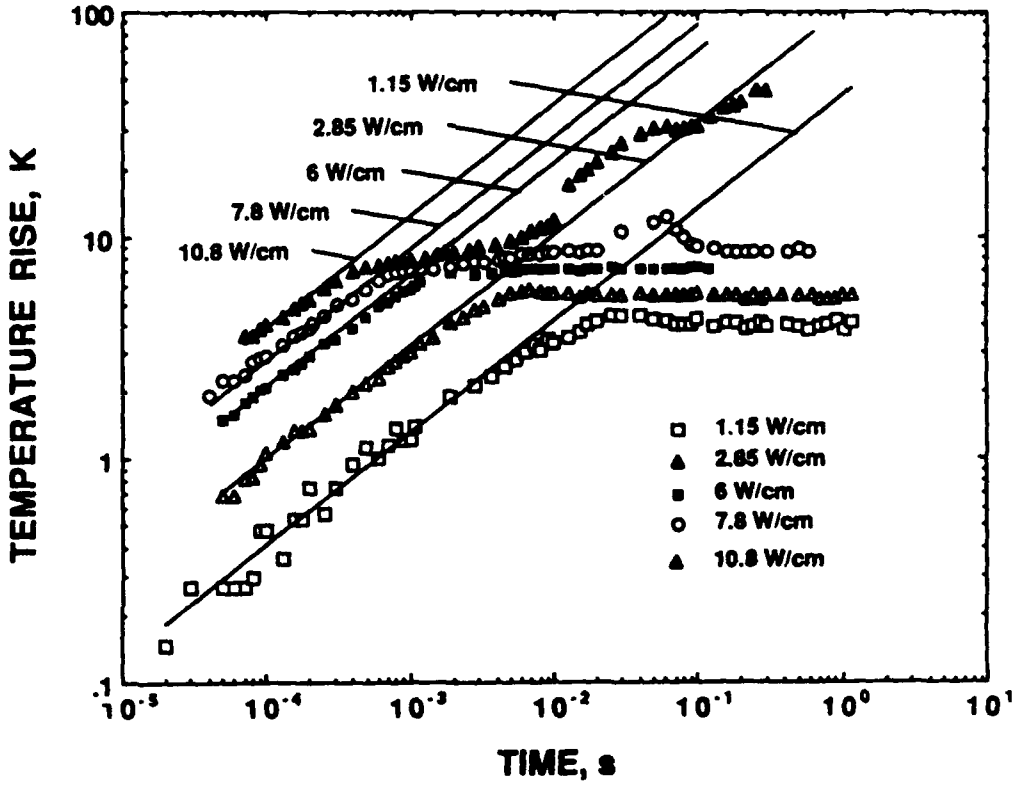

Figure 7. Results of transient heat transfer experiments from a carbon thin film to LH_2 for heat fluxes ranging from 1.15 to 10.8 W/cm².

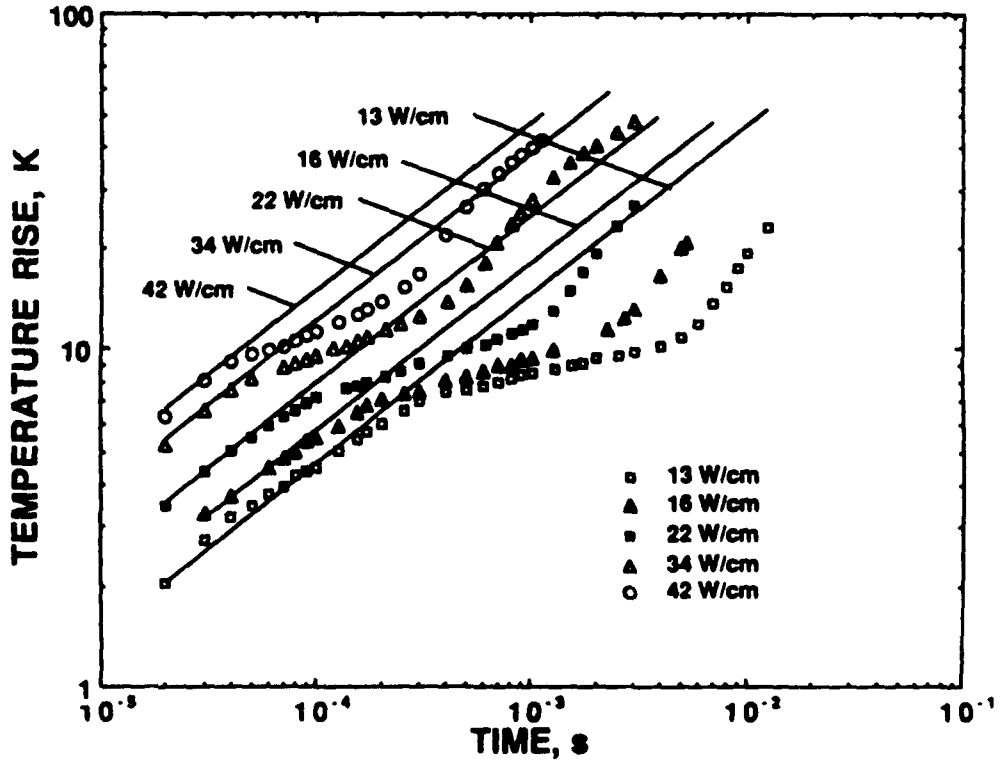

Figure 8. Results of transient heat transfer experiments from a carbon thin film to LH_2 for heat fluxes ranging from 13 to 42 W/cm².

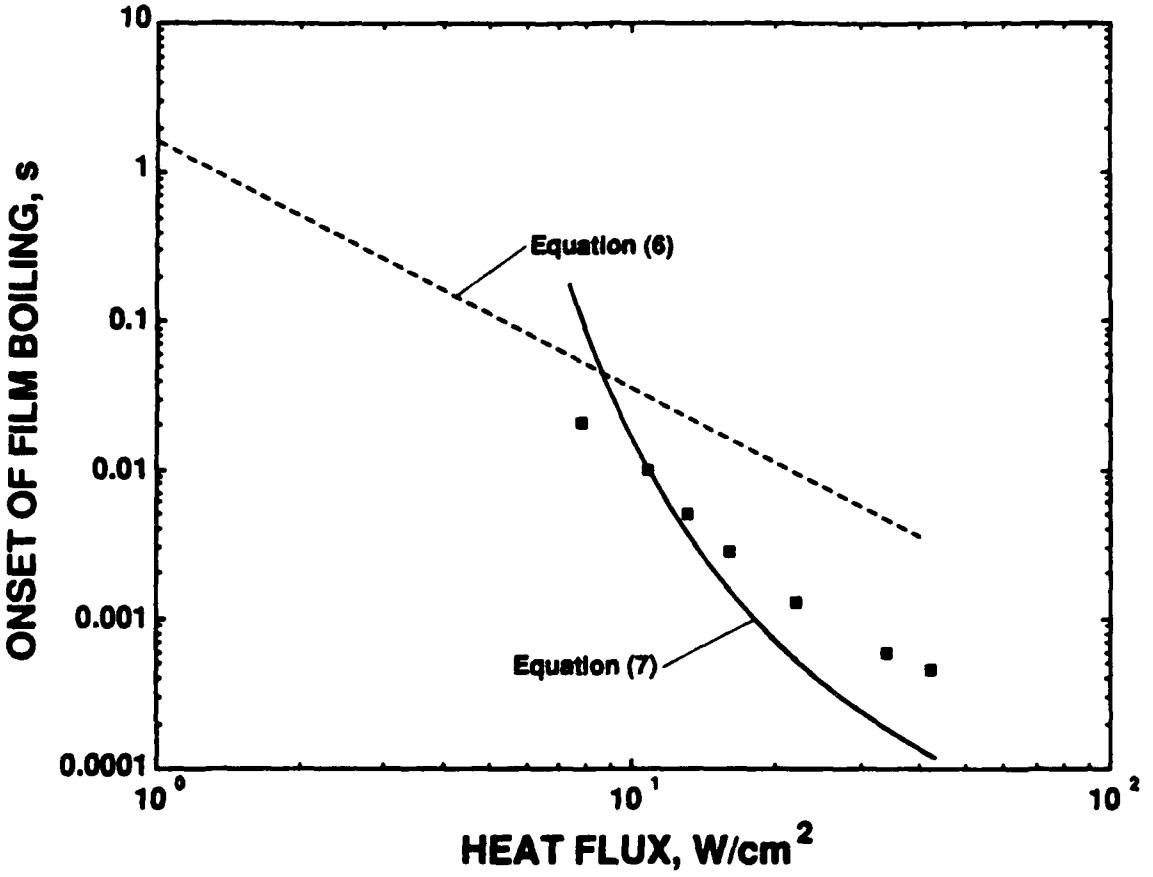

Figure 9. Experimental data from transient heat transfer experiments using a carbon film in LH_2 which show the time of transition to film boiling for various applied heat fluxes. The data are compared to Equations (6) and (7) which predict the time for the onset of film boiling.

compute t_f from the time of end of the conduction period rather than from the time of the beginning of the application of power:

$$t_f = t_c + \gamma^2 \left[\frac{k}{\rho c}\right] \left[\frac{L}{q - q_{cr}}\right]^2 . \qquad (7)$$

The carbon film data points show reasonable agreement with Equation (6). The slight curvature in the slope of the data points at the higher heat fluxes is similar to the curved line of Equation (7) in Figure 9. The agreement may be enhanced by optimizing γ.

Observations in liquid nitrogen. Sinha et al. [4] report that following stepped power inputs, transitions to stable film boiling in LN_2 on horizontal 0.102 mm Pt wires were observed for heat fluxes as low as 40% of the maximum steady-state heat flux for film boiling. Tsukamoto, et al. [5] photographed premature film boiling resulting from stepped power inputs to a horizontal 0.05 mm Pt wire at 50% of the steady-state burnout heat flux. We recorded experiments in LN_2 on high-speed video which used a 0.38 mm wide, unsupported Pt ribbon. We observed the development of periodic bubbles, which coalesced and enveloped the ribbon, as well as the corresponding transitions to film boiling. These transitions are unusual because they occur at heat fluxes from 2 to 10 W/cm^2, which normally support steady nucleate boiling. [1] We assume similar behavior for liquid hydrogen, due to the similarity in results.

Liquid hydrogen results. We found that early and unpredictable transitions to film boiling in LH2 occurred using unsupported Pt ribbons with widths of 0.178 mm to 1.524 mm. The data, shown in Figure 10, do not follow the Q^{-2} dependence predicted by Equation (6) and exhibit widely varying transition times for the same heat flux. The heater width is on the order of the width of the average nucleate boiling bubble. An average bubble size, between 0.246 to 0.52 mm, and time of departure from the heater surface, between 5 to 36 ms, has been reported by Thome and Davey, [9] for mixtures of LN_2 and LAr, and by Bewilogua et al. [10], for bubble formation in boiling hydrogen. In the experiments of Sinha et al. [4] and of Tsukamoto et al. [5] the Pt wire diameters, respectively 0.102 mm and 0.05 mm, were smaller than the average bubble size.

Premature film boiling might be a manifestation of nonuniform heating promoted by a positive temperature coefficient of resistance combined with the small width of the heater. In particular, if the width of a heater is nearly as small as a nucleate boiling bubble, a small number of bubbles might effectively insulate a segment of heater and cause the temperature of that segment to rise above the average. The local Joule heating and temperature would then increase further. The absence of a nearby heat sink or substrate would encourage this process to continue.

Hydrodynamic instability. We apply the Taylor-Helmholtz analysis to our data. A harmonic, surface-tension wave on the vapor-liquid interface with a small amplitude perturbation may be described by [11]

$$z = z_0 e^{bt} \cos(mx) . \qquad (8)$$

The stability of the system is determined by b. There is a dominant wavelength which corresponds to the maximum value of b. A maximum value of b describes when the minimum thickness of vapor required for stable film boiling has been reached [11]. The maximum

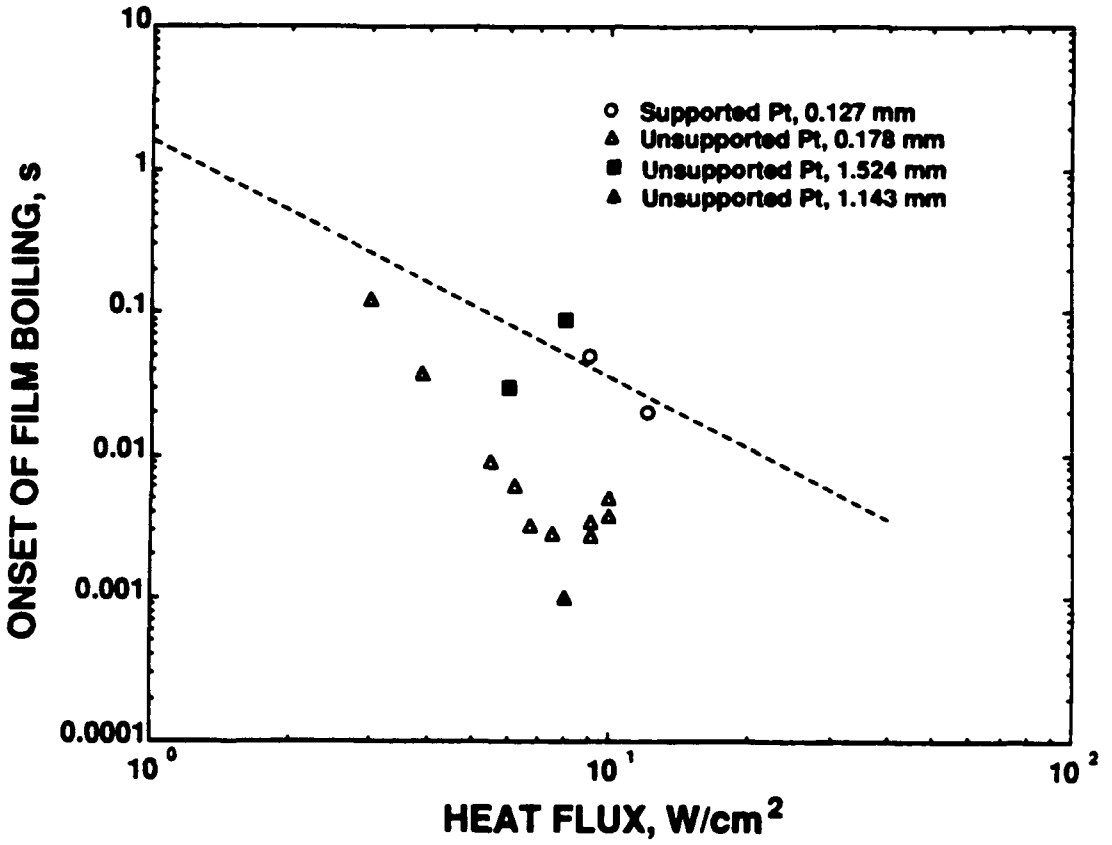

Figure 10. Experimental data for unsupported Pt films exposed to LH_2 on both sides compared to prediction for onset of film boiling presented in Equation 6.

value of b, 44.5 s^{-1}, corresponds to a dominant wavelength of 20 mm. Comparing the corresponding time of 22.5 ms to Figure 10 shows that many transitions occurred at even earlier times, a reasonable indication that stable film boiling has been reached in those cases. Other factors which may account for premature film boiling include: (1) reduced surface tension with a vertical test section, and (2) the width of the Pt ribbon, many times smaller than the dominant wavelength, which encourages the coalescence of the nucleate boiling bubbles.

Temperature excursions in substrate-mounted Pt devices. The data of Figure 11, for substrated-mounted Pt devices in LH_2 differ from those of the carbon film and from the unsupported Pt foil in LH_2 in two respects: (1)a large temperature overshoot at the onset of nucleate boiling, and (2)a brief temperature excursion preceding the overshoot. These phenomena are associated with the use of narrowest (0.127 mm wide) serpentine pattern Pt heater mounted on a quartz substrate. This heater also had a number of imperfections, such as pinholes and ragged cut edges, which could promote the formation of a hot spot as discussed earlier. The temperature excursion can be explained by the development of such a film boiling spot, and the substrate acted as a poor heat sink imperfectly connected to the foil through the epoxy adhesive. The relatively large temperature overshoot could also be related to this poor thermal coupling.

4.3 Estimation of Heater Temperature Rise During Film Boiling

For heat fluxes greater than the nucleate boiling maximum, a period of extraordinarily low heat transfer resistance, metastable nucleate boiling ends with a rise in temperature toward the film boiling level. For practical applications it can be assumed that the heat transfer coefficient falls immediately to a value of 30 to 50 $mW/(cm^2 \cdot K)$, corresponding to film boiling [8], and the thermal properties of solid materials control temperature rise. Heaters with very small mass, such as the Pt ribbons, jump quite abruptly to steady-state film boiling temperatures.

The solid lines for heat fluxes of 13 and 42 W/cm^2 in Figure 12 show the results of our calculation, using Equation (1), of temperature rise during the transition where conduction into the quartz substrate controls the temperature rise and the effect of the fluid is neglected. The curvature is due to the large variation of solid thermal properties. These conduction curves would extend upward indefinitely and therefore should be discontinued where they intersect the steady state film boiling temperature.

4.4 Transient Conduction Heat Transfer from Pt Ribbons

Figures 13 – 16 show temperature rise versus time for heat transfer to saturated LH_2 from a Pt ribbon 1.778×10^{-2} cm wide, 3.48 cm long, and 4 μm thick, exposed to the liquid on both sides. Stepped power inputs were 3, 6, 7, and 9 W/cm^2. Conduction heat transfer gives way to boiling heat transfer at about 1.2 ms at 3 W/cm^2 (Figure 13), and the transition time recedes as the power increases (Figures 14 – 16). At 9 W/cm^2 the transition to boiling begins at about 0.4 ms. In order to describe the conduction period realistically, the computations used temperature dependent liquid and solid properties, and the time dependent power as determined experimentally. The resulting computations, shown as the solid lines in Figures 13 – 16, agree well with measurements made during periods when the power is not constant; the variations in power are reflected in the different slopes at early times.

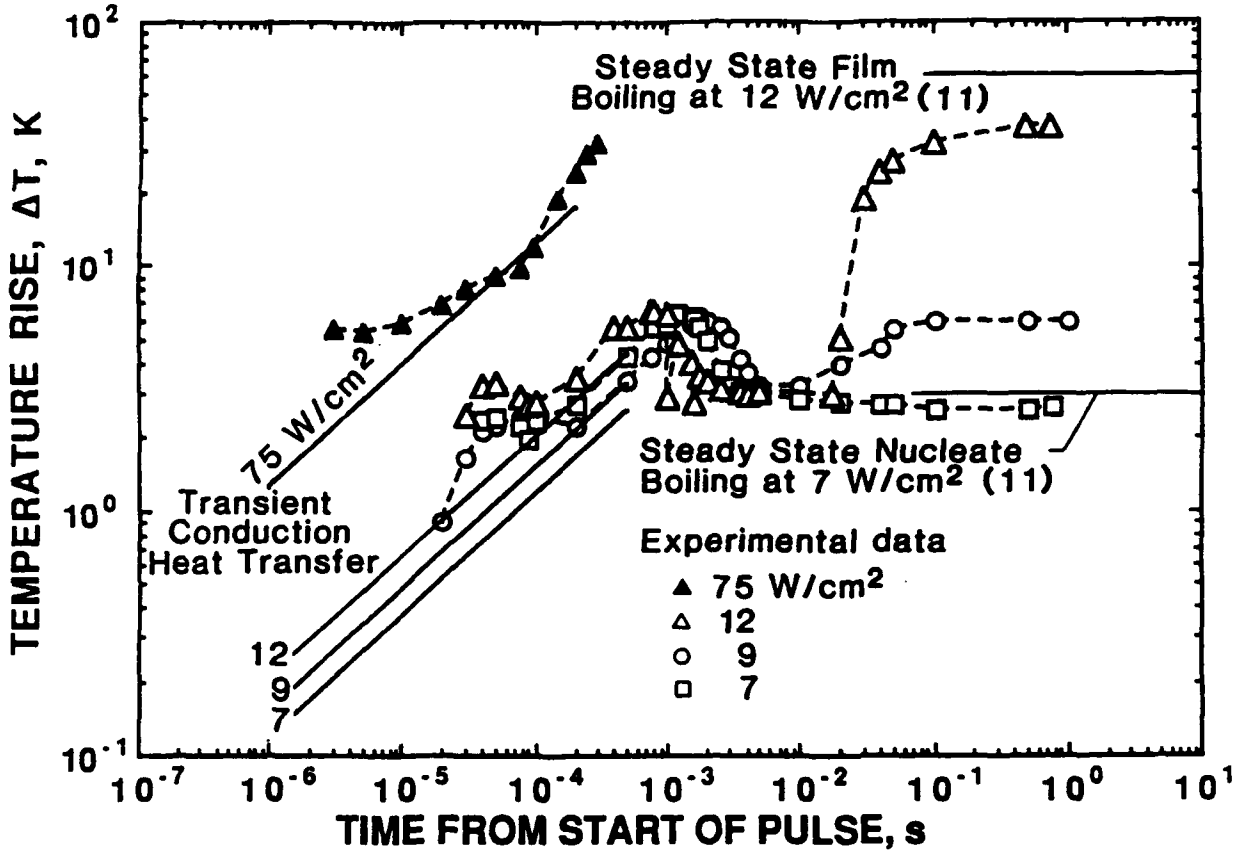

Figure 11. Results of transient heat transfer to supported Pt foil in LH_2.

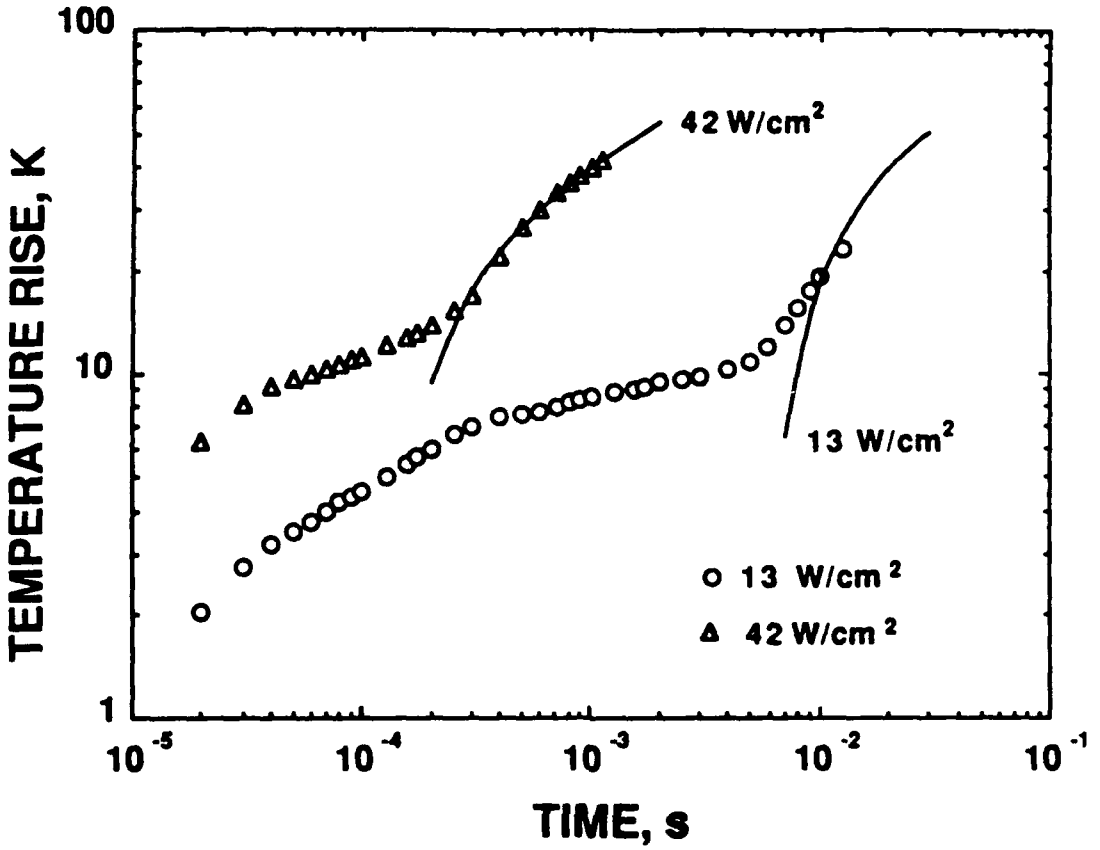

Figure 12. Comparison of data to calculation, based on Equation 1, of temperature rise during transition to film boiling of a substrate-mounted carbon film in LH_2

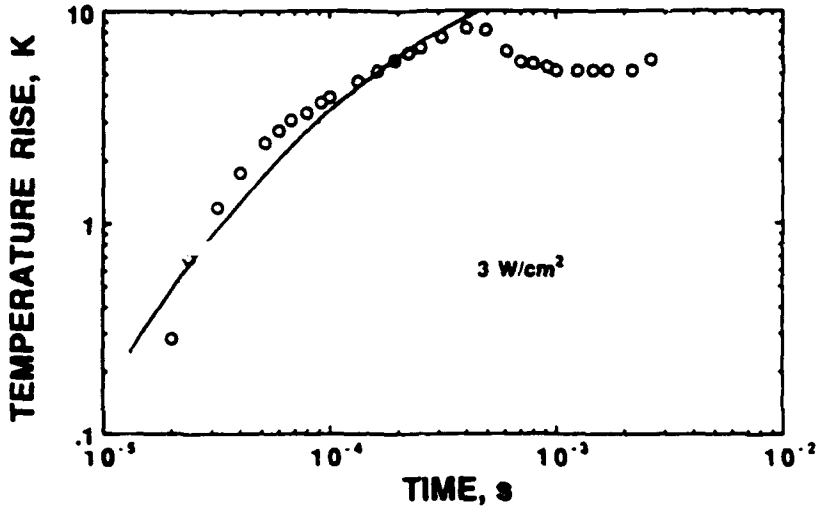

Figure 13. Comparison of experimental data for unsupported Pt ribbon to computation with temperature dependent solid and liquid properties and the time dependent power for power input of 3 W/cm².

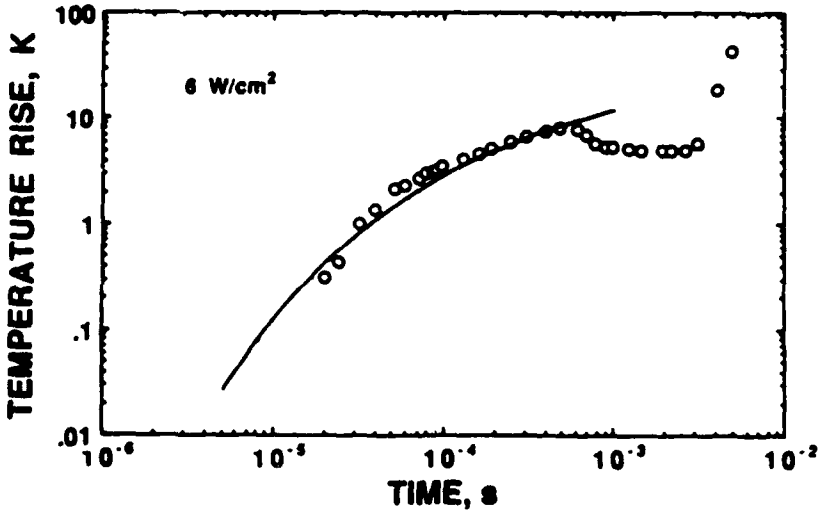

Figure 14. Comparison of experimental data for unsupported Pt ribbon to computation with temperature dependent solid and liquid properties and the time dependent power for power input of 6 W/cm².

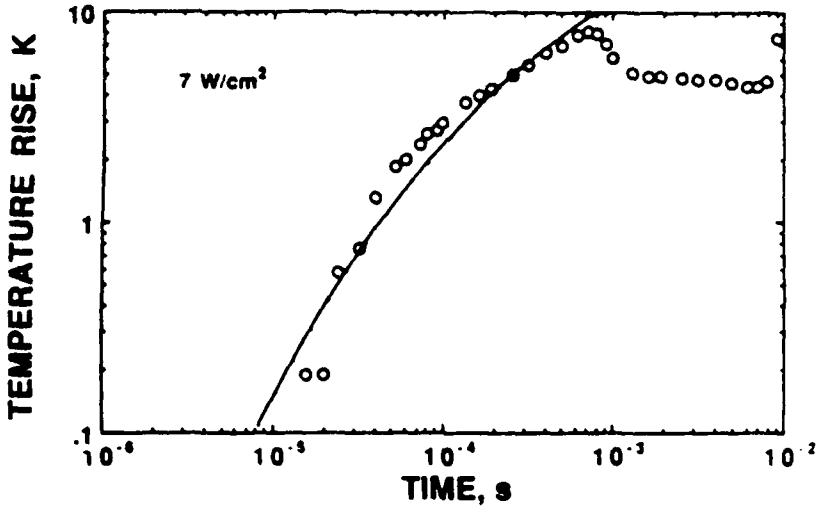

Figure 15. Comparison of experimental data for unsupported Pt ribbon to computation with temperature dependent solid and liquid properties and the time dependent power for power input of 7 W/cm².

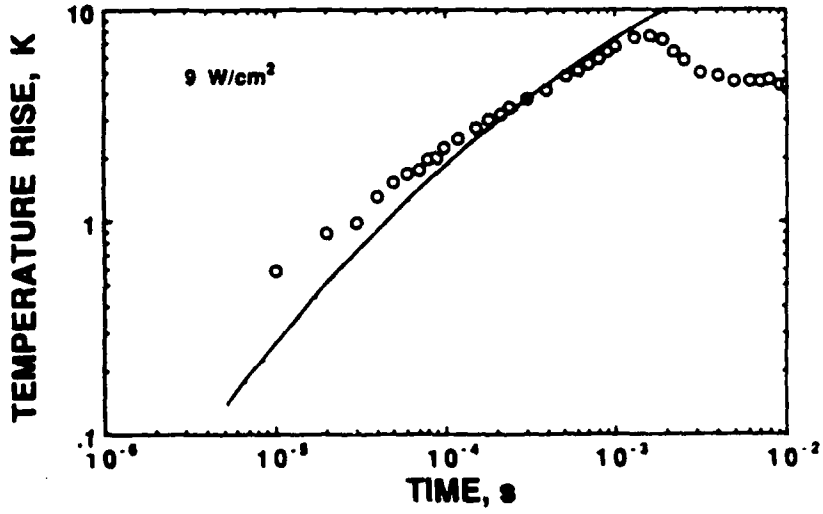

Figure 16. Comparison of experimental data for unsupported Pt ribbon to computation with temperature dependent solid and liquid properties and the time dependent power for power input of 9 W/cm².

5. SUMMARY AND CONCLUSIONS

We studied transient heat transfer to carbon film and Pt foil devices submerged in LH_2, with emphasis placed on the onset of conduction and of film boiling. The experimental results are summarized in Table 1 for each heater/thermometer used. A solution of Equation (1) for the transient conduction differential equation for a massless heater bounded by a solid substrate on one side and liquid on the other was used to analyze the carbon film data. Representation of the unsupported ribbon data required a new solution, which is presented in this paper as Equation (2). Except in cases of premature film boiling, the empirical expression of Schmidt [2], Equation (6), and the modification in Equation (7) predict t_f at the higher heat fluxes. Premature film boiling can be related to the narrowness 1.524 mm or less of the heaters relative to the size of nucleate boiling bubbles, irregularities in the heater material, and a positive coefficient of electrical resistance.

Table 1. Summary of Transient Heat Transfer to Liquid Hydrogen

Type of Heater	Transient Conduction Period	Equation for Trans. Conduction	Time to Onset of Film Boiling	Equation for Onset of Film Boiling	Comments or Exceptions
Carbon Thin Film	10 μs to 20 ms	Eq (1)	10 ms for 10.8 W/cm^2	Eqs (6) and (7)	Critical Heat Flux 7.8 W/cm^2
Pt Foil Ribbons Boiling	10 μs to 1 ms	Eq (2)	3 ms for 7 W/cm^2	Eqs (6) and (7)	Premature Film related to narrow heaters
Pt Foil on Quartz	1 μs to 5 ms	Eq (1)	20 ms for 12 W/cm^2	(not studied)	Temp. excursions due to hot spots, substrate effects

6. ACKNOWLEDGEMENTS

The authors wish to recognize the contributions of N.V. Frederick who designed, constructed, and tested important electronic components for this study. His assistance has been invaluable and is greatly appreciated.

Work performed under WPAFB MIPR contract number FY1455–89–N0604.

7. NOMENCLATURE

A	surface area, cm
b	growth parameter
c	specific heat, J/(g K)
k	thermal conductivity, W/(cm K)
L	heat of vaporization, J/g
m	wave number $= 2\pi/\lambda$
Q	applied heat flux, W/(cm² s)
Q_{cr}	critical heat flux, W/(cm² s)
q	heat flux per unit volume, W/cm³
R_s	resistance of standard resistor, Ω
R_t	resistance of test resistor, Ω
t	time s
t′	dimensionless time $= t\alpha_s/\delta^2$
t_c	time of conduction period, s
t_f	time of onset of film boiling, s
T	heater surface temperature, K
T′	dimensionless temperature $= T\alpha_s/(q\delta^2)$
V_t	voltage across the test section, V
V_s	voltage across the standard resistor, V
x	length of fluid–vapor interface, cm
z	amplitude of perturbation, cm
z_0	perturbation constant
α	thermal diffusivity $= k/(\rho c)$, cm²/s
β	dimensionless parameter $= (k_s/k_f)(\alpha_s/\alpha_f)$
δ	ribbon thickness, cm
γ	fit factor
ρ	density, g/cm³
λ	wavelength, cm
σ	surface tension, dyn/cm
θ	integration variable for time

$_{v,l}$	denote vapor, liquid
$_{s,f}$	denote solid, fluid
erfc	complementary error function

8. REFERENCES

[1] W. G. Steward, Transient Helium Heat Transfer Phase I – Static Coolant, Int. J. Heat Mass Transfer, 21:863 (1978).

[2] C. Schmidt, Transient Heat Transfer into a Closed Small Volume of Liquid or Supercritical Helium, Cryogenics, 28:585 (1988).

[3] O. Tsukamoto, T. Uyemura, and Y. Ishida, Observation of Bubble Formation Mechanism of Liquid Helium Subjected to Transient Heating, Proc. Eighth Int. Cryog. Eng. Conf., Butterworth, Guildford, UK (1980), p. 251.

[4] D. N. Sinha et al., Premature Transition to Stable Film Boiling Initiated by Power Transients in Liquid Nitrogen, Cryogenics, 19:225 (1979).

[5] O. Tsukamoto, T. Uyemura, and T. Uyemura, Observation of Bubble Formation Mechanism of Liquid Nitrogen Subjected to Transient Heating, Advances in Cryogenic Engineering, Vol.25, (1980), p. 476.

[6] K. B. Martin and V. J. Johnson, Safety Instruction and Safety Guide for Handling Gaseous and Liquid Hydrogen at the Boulder Laboratories, Nat. Bur. Stand. (U.S.) Monogr. CM–4; (1960).

[7] P. J. Giarratano and W. G. Steward, Transient Forced Convection Heat Transfer to Helium During a Step in Heat Flux, J. Heat Transfer, 105:350 (1983).

[8] E. G. Brentari, P. J. Giarratano, and R. V. Smith, Boiling Heat Transfer or Oxygen, Nitrogen, Hydrogen, and Helium, Nat. Bur. Stand. (U.S.) Tech. Note; 317 (1965).

[9] J. R. Thome and G. Davey, Bubble Growth Rates in Liquid Nitrogen, Argon and Their Mixtures, Int. J. Heat Mass Transfer, 24:89 (1981).

[10] L. Bewilogua, R. Knoner and H. Vinzelberg, Studies on Bubble Formation in Low Boiling Liquids, Cryogenics, 10:69 (1970).

[11] S. Van Stralen and R. Cole, Boiling Phenomena, Hemisphere, Washington (1979), p. 615.

Appendix A

TRANSIENT CONDUCTON HEAT TRANSFER – FLAT PLATE HEATER ON A SOLID SUBSTRATE WITH LIQUID COOLANT

Assume:

1. Infinite flat plate heater in the x – y plane at z = 0. Note: If the substrate were finite in the –z direction one would have to make an assumption about heat transfer at a bottom boundary. The results are the same until a temperature wave penetrates the finite substrate.

2. Heater has zero thickness.

3. Stagnant liquid hydrogen lies above the plate ($z > 0$); no forced convection is present.

4. A solid substrate lies below the plate ($z < 0$).

5. Times of concern are short enough that thermal convection currents are not established and no bubbles have formed. This would mean non–equilibrium of phases (superheating) in cases where $T_f > T_{saturation}$.

6. Heating is at constant volume, i.e. no work of compression.

7. Radiation heat transfer is much less than conduction heat transfer.

8. Fluid and solid properties are constant.

The Fourier heat conduction equation in 1 dimension is presented for the following cases:

A. Solid Substrate (subscript $_s$)

$$\frac{\partial T_s}{\partial z^2} = \frac{1}{\alpha_s}\frac{\partial T_s}{\partial \theta} \qquad z \leq 0, \qquad (1)$$

where T_s = temperature of substrate at z and time θ
=temperature before disturbance.

θ = time

α_s = thermal diffusivity = $\dfrac{K_s}{\rho_s C_{ps}}$

K_s = thermal conductivity

ρ_s = density

C_{ps} = specific heat

Boundary Conditions for the Substrate

$$T_s(z,\theta) = 0 \qquad (2)$$

$$\lim_{z \to \infty} T_s(z,\theta) = 0 \tag{3}$$

$$\rho_s = K_s \left[\frac{\partial T}{\partial z}\right]_{0,\theta} \quad \text{the part of the heater power being dissipated in the substrate.} \tag{4}$$

B. Conduction Equation for the Fluid

$$\frac{\partial^2 T_f}{\partial z^2} = \frac{1}{\alpha_f}\frac{\partial T_f}{\partial \theta} \qquad z \geq 0 \tag{5}$$

where T_f = temperature of fluid at z,
θ = temperature before disturbance.

Boundary Conditions for the Fluid

$$T_f(z,0) = 0 \tag{6}$$

$$\lim_{z \to \infty} T_f(z,\theta) = 0 \tag{7}$$

$$P_f = -K_f\left[\frac{\partial T}{\partial z}\right]_{0,\theta} \quad \text{part of the heater power being dissipated in the fluid.} \tag{8}$$

C. Condition at the substrate/heater/liquid interface:

$$P = P_f + P_s \quad \text{total heater power — known parameter} \tag{9}$$

$$T_s(0,\theta) = T_f(0,\theta) \tag{10}$$

D. Solution for the Substrate

Laplace transform with respect to θ

$$\frac{\partial^2 t}{\partial z^2}(z,s) = \frac{1}{\alpha_s}\left[st(z,s) - T(z,0)\right] . \tag{11}$$

From B.C. #2 $T(z,0) \to 0$,

where $t(z,s) = L[T(z,\theta)]$

s = the Laplace transform parameter.

The solution of (11) is

$$t = C_1 e^{z\sqrt{s/\alpha_s}} + C_2 e^{-z\sqrt{s/\alpha_s}} .$$

From B.C. #3 $C_2 = 0$. Therefore,

$$t = C_1 e^{z\sqrt{s/\alpha_s}} . \tag{12}$$

Transform B.C. #4:

$$\frac{P_s}{s} \quad K_s \left[\frac{\partial t}{\partial z} \right]_{0,s} .$$

Then from Equation (12),

$$\frac{P_s}{s} = K_s C_1 \sqrt{s/\alpha_s}\, e^{z\sqrt{s/\alpha_s}} \Big|_{z=0}$$

or

$$C_1 = \frac{P_s}{s} \frac{1}{K_s} \sqrt{s/\alpha_s} .$$

Therefore,

$$t = \frac{1}{s} \left[\frac{P_s}{K_s} \sqrt{\alpha_s/s}\, e^{z\sqrt{s/\alpha_s}} \right]^* . \tag{13}$$

*It is assumed in the following development of equations that P_s is constant. Further explanation is provided in the addendum following this appendix.

Use the following transform relations:

$$L\left[\frac{1}{\sqrt{\pi\theta}} e^{z^2/4\alpha_s\theta} \right] = \frac{1}{\sqrt{s}} e^{-z\sqrt{s/\alpha_s}} \tag{14}$$

and

$$L\left[\int_0^\theta F(\tau)\, d\tau \right] = \frac{1}{s} f(s) . \tag{15}$$

Then combining Equations (13) and (14) yields the following expression:

$$t = \frac{1}{s} L \left[\frac{P_s}{K_s} \sqrt{\alpha_s/(\pi\theta)}\, e^{-z^2/(4\alpha_s\theta)} \right] .$$

From Equation (15)

$$t = L\left[\int_0^{\theta} \frac{P_s}{K_s}\sqrt{\alpha_s/(\pi\tau)}\, e^{-z^2/(4\alpha_s\tau)}\, d\tau\right]$$

(where τ = dummy variable).

Therefore,

$$T_s = \frac{P_s}{K_s}\sqrt{\alpha_s/\pi}\int_0^{\theta} \frac{e^{-z^2/(4\alpha_s\tau)}}{\sqrt{\tau}}\, d\tau\,. \tag{16}$$

A change of variables is now introduced:

Let $\lambda = \dfrac{z}{2\sqrt{\alpha_s\tau}}$.

Therefore $\dfrac{1}{\sqrt{\tau}} = \dfrac{2\sqrt{\alpha_s\lambda}}{z}$, and $\tau = \dfrac{z^2}{4\lambda^2\alpha_s}$.

Hence, $\quad d\tau = \dfrac{2\ z^2 d\lambda}{4\ \lambda\ \alpha_s} = \dfrac{1}{2}\dfrac{z^2}{\lambda^3}\dfrac{d\lambda}{\alpha_s}$.

Also,

$\tau = 0 \Rightarrow \lambda = \infty$,

$\tau = \theta \Rightarrow \lambda = \dfrac{z}{2\sqrt{\alpha_s\theta}}$.

The following expression can be derived:

$$T_s = \frac{P_s}{K_s}\sqrt{\alpha_s/\pi}\int_{\infty}^{\frac{z}{2\sqrt{\alpha_s\theta}}} e^{-\lambda^2}\left[\frac{2\sqrt{\alpha_s}}{z}\right]\lambda\left[\frac{1}{2}\frac{z^2}{\lambda\ \alpha_s}\right] d\lambda\,,$$

or

$$T_s = \frac{P_s}{K_s}\frac{z}{\sqrt{\pi}}\int_{\frac{z}{2\sqrt{\alpha_s\theta}}}^{\infty} \frac{e^{-\lambda^2}}{\lambda}\, d\lambda\,. \tag{17}$$

Now we perform an integration by parts: $\int u dv = uv - \int v du$.

Let $dv = \frac{d\lambda}{\lambda^2}$ and $v = \frac{1}{\lambda}$

$u = e^{-\lambda^2}$ and $du = -2\lambda e^{-\lambda^2} d\lambda$.

Then,

$$T_s = \frac{P_s}{K_s}\frac{z}{\sqrt{\pi}}\left[\left[-\frac{e^{-\lambda^2}}{\lambda}\right]_{\frac{z}{2\sqrt{\alpha_s\theta}}}^{\infty} - 2\int_{\frac{z}{2\sqrt{\alpha_s\theta}}}^{\infty} e^{-\lambda^2} d\lambda\right],$$

or

$$T_s = \frac{P_s}{K_s}\left[\frac{2\sqrt{\alpha_s\theta}}{\sqrt{\pi}} e^{\frac{-z^2}{4\alpha_s\theta}} - \frac{2z}{\sqrt{\pi}}\underbrace{\int_{\frac{z}{2\sqrt{\alpha_s\theta}}}^{\infty} e^{-\lambda^2} d\lambda}_{z\cdot \mathrm{erfc}\frac{z}{2\sqrt{\alpha_s\theta}}}\right].$$

Therefore,

$$T_s = \frac{P_s}{K_s}\left[2\sqrt{\alpha_s\theta/\pi}\, e^{-z^2/4\alpha_s\theta} - z\cdot\mathrm{erfc}\left[\frac{z}{2\sqrt{\alpha_s\theta}}\right]\right] \qquad (18)$$

at $z \leq 0$.

Substrate Surface Temperature ($z = 0$)

$$T_s(0,\theta) = 2\frac{P_s}{\sqrt{\pi}}\frac{\sqrt{\alpha_s}}{K_s}\sqrt{\theta}\,. \qquad (19)$$

E. Solution for the Fluid

By starting with eq. (5) and boundary conditions (6), (7), and (8) we get the same solution as (18) except the properties are fluid properties and the power is P_f.

$$T_f = \frac{P_f}{K_f}\left[2\sqrt{\alpha_f\theta/\pi}\, e^{-z^2/4\alpha_f\theta} - z\cdot\mathrm{erfc}\left[\frac{z}{2\sqrt{\alpha_f\theta}}\right]\right] \qquad (20)$$

at $z \geq 0$,

or

$$T_f = \frac{2}{\sqrt{\pi}} \left[\frac{\sqrt{\alpha}}{K}\right]_f P_f \sqrt{\theta} \left[e^{-x^{*2}} - \sqrt{\pi} \left[x^* \operatorname{erfc} x^* \right] \right] , \quad x^* = \frac{z}{2\sqrt{\alpha_f \theta}} .$$

and at the liquid surface the temperature is:

$$T_f(0,\theta) = \frac{2P_f}{\sqrt{\pi}} \frac{\sqrt{\alpha_f}}{K_f} \sqrt{\theta} . \tag{21}$$

F. Solution in terms of P and θ

At the interface $P_s + P_f = P$, and $T_s(0,\theta) = T_f(0,\theta) = T(0,\theta)$. Therefore, from Equations (19), and (21):

$$P = \frac{T(0,\Theta)}{2} \sqrt{\pi/\theta} \left[\frac{K_s}{\sqrt{\alpha_s}} + \frac{K_f}{\sqrt{\alpha_f}}\right] . \tag{21a}$$

ADDENDUM – PROOF THAT P_s AND P_f ARE CONSTANT

From Equation (12) we know that $t = C_1 e^{z\sqrt{s/\alpha_s}}$ for the substrate $(z < 0)$.

For the fluid $t = C_3 e^{-z\sqrt{s/\alpha_f}}$, $(z > 0)$. (A)

At $z = 0$ the temperature of the substrate = temperature of liquid, therfore $C_1 = C_3 = C$.

$$P_s = s\, C\, K_f \sqrt{s/\alpha_f} ,$$

and

$$P_f = s\, C\, K_s \sqrt{s/\alpha_s} .$$

Therefore,

$$\frac{P_s}{P_f} = \frac{K_f}{K_s} \sqrt{\frac{\alpha_s}{\alpha_f}} = (\text{const})_1 ,$$

$$P = P_f + P_s = (\text{const})_2 \quad \text{(given)} , \tag{B}$$

$$P = P_f(1 + \text{const}_1) = (\text{const})_2 .$$

$$P_f = \frac{(\text{const})_2}{1 + (\text{const})_1} = (\text{const})_3.$$

Similarily $P_s = (\text{const}_4)$.

It is not necessary to know that P_s is constant. Using condition (A) above and Equation (22) gives the same result.

Appendix B

TRANSIENT CONDUCTION HEAT TRANSFER FROM A RIBBON HEATER WITH INTERNAL HEAT GENERATION

The unsteady state conduction equation is

$$\nabla^2 T + \frac{q}{K} = \frac{1}{\alpha}\frac{\partial T}{\partial t}, \qquad 1)$$

where
- q = generated heat flux/volume
- k = thermal conductivity
- α = thermal diffusivity
- T = temperature – initial temperature
- t = time

A. Development of equations for the solid

Equation (1) for the solid is:

$$\frac{\partial^2 T}{\partial y^2} + \frac{q}{K_s} = \frac{1}{\alpha_s}\frac{\partial T}{\partial t}. \qquad (2)$$

Boundary Conditions:

$$T(y,0) = 0 \qquad \text{(initial condition)}. \qquad (3)$$

$$\frac{\partial T}{\partial t}(0,t) = 0 \qquad \text{(symmetry)}.$$

Change to dimensionaless variables:

Let $y' = \frac{y}{\delta}$ (dimensionless space variable).

To write Equation (2) in dimensionless terms, the following must exist:

$$\frac{\partial^2 T}{\partial y^2} = \frac{q}{K_s} = \frac{T}{y^2}.$$

Let $T' = \frac{T}{A}$.

Then $\frac{T'A}{(y'\delta)^2}$ [=] $\frac{q}{K_s}$ or $A = \frac{q\delta^2}{K_s}$.

Let $t' = \frac{t}{B}$. Then,

$$\frac{1}{\alpha_s}\frac{\partial T}{\partial t} \; [=] \; \frac{1}{\alpha}\frac{\Delta T'}{B t'} \; [=] \; \frac{q}{K_s} .$$

Since $\frac{T'}{t'}$ [=] 1 and $\gamma = \frac{q\delta^2}{K_s}$,

$$\frac{1}{\alpha}\frac{q\delta^2}{K_s}\frac{1}{B} = \frac{q}{K_s},$$

where $B = \frac{\delta^2}{\alpha}$.

Recap: The dimensionless space coordinate, temperature, and time are:

$$y' = \frac{y}{\delta} \quad \text{or} \quad y = \delta y' \tag{4}$$

$$T' = \frac{TK_s}{q\delta^2} \quad \text{or} \quad T = T'\frac{q\delta^2}{K_s} \tag{4}$$

$$t' = \frac{t\alpha_s}{\delta^2} \quad \text{or} \quad t = \frac{t'\delta^2}{\alpha_s} . \tag{4}$$

When these variables are substituted into Equation (2) we have the dimensionless equation for the solid:

$$\frac{\partial^2 T'}{\partial y'^2} + 1 = \frac{\partial T'}{\partial t'} \tag{5}$$

B. Development of equations for the liquid

The conduction equation for the liquid lacks the heat generation term

$$\frac{\partial^2 T}{\partial y^2} = \frac{1}{\alpha_l}\frac{\partial T}{\partial t} \tag{6}$$

The dimensionless equation for the liquid is

$$\frac{\partial^2 T'}{\partial y'^2} = \frac{\alpha_s}{\alpha_l}\frac{\partial T'}{\partial t'} . \tag{7}$$

Boundary condition for the liquid

$$T(\infty, t) = 0 . \tag{8}$$

C. Coupling the equations

To couple Equations (2) and (6):

$$\text{at } y = \delta/2 \quad T_s\left[\delta/2,t\right] = T_l\left[\delta/2,t\right] , \tag{9}$$

$$\text{and } K_s\left[\frac{\partial T}{\partial y}\right]_{y = \delta/2} = K_l\left[\frac{\partial T}{\partial y}\right]_{y = \delta/2} . \tag{10}$$

Or, in terms of the dimensionless variables:

$$y' = 1/2 \quad T_s'(1/2,t') = T_l'(1/2,t') \tag{9'}$$

$$\text{and } K_s\left[\frac{\partial T'}{\partial y'}\right]_{y'=1/2} = K_l\left[\frac{\partial T'}{\partial y'}\right]_{y'=1/2} \tag{10'}$$

D. Transformed Solution

Laplace Transform

$$\text{Solid: } \frac{\partial^2 \tau}{\partial y'^2} + \frac{1}{s} = s\tau - \tau(y',0)$$

Initial condition. $\tau(y',0) = 0$)

$$\frac{\partial^2 \tau'}{\partial y'^2} - s\tau = -\frac{1}{s}$$

where τ is the Laplace–transformed temperature
s is the Laplace transform variable

Particular Solution $\tau_p = \frac{1}{s^2}$.

Homogeneous Solution $\tau_c = C_3 e^{\sqrt{s}y'} + C_4 e^{-\sqrt{s}y'}$.

Total solution $$\tau = C_3 e^{\sqrt{s}y'} + C_4 e^{-\sqrt{s}y'} + \frac{1}{s^2} . \tag{11}$$

The symmetry B.C. $\rightarrow \left[\frac{\partial \tau}{\partial y'}\right]_{y' = 0}$.

From Equation (11), $\left[\frac{\partial T}{\partial y'}\right]_{y'=0} = \left[C_3\sqrt{s}e^{\sqrt{s}y'} - C_4\sqrt{s}e^{-\sqrt{s}y'}\right]_{y'=0}$,

which gives

$$C_3 = C_4 .$$

Therefore,

$$\tau = C_3\left[e^{\sqrt{s}y'} + e^{-\sqrt{s}y'} \right] + \frac{1}{s^2} . \tag{12}$$

For the liquid $\frac{\partial^2 \tau}{\partial y'^2} = \frac{\alpha_s}{\alpha_1}\left[s\tau - \tau(y',\cancel{0}0)\right]$

$$\tau = C_1 e^{\sqrt{\alpha_s/\alpha_1}\sqrt{s}y'} + C_2 e^{-\sqrt{\alpha_s/\alpha_1}\sqrt{s}y'} ,$$

and

$$\tau(\alpha,t) = 0 \text{ or } \tau(\infty,s) = 0 \longrightarrow C_1 = 0 .$$

Therefore,

$$\tau = C_2 e^{-\sqrt{s}y'\sqrt{\alpha_s/\alpha_1}} . \tag{13}$$

C_3 and C_2 can be evaluated from Equations (12) and (13) and the coupling condition from Equation (9′) at $y' = 1/2$:

$$\left[e^{\sqrt{s}/2} + e^{-\sqrt{s}/2}\right] + \frac{1}{s^2} = C_2 e^{-\sqrt{s}/2\sqrt{\alpha_s/\alpha_1}} . \tag{14}$$

To use Equation (10′), differentiate Equations (12) and (13) and evaluate at $y' = 1/2$:

$$C_3 \frac{K_s}{K_1}\sqrt{\alpha_s/\alpha_1}\sqrt{s}\left[e^{\sqrt{s}/2} + e^{-\sqrt{s}/2}\right] = -C_2\sqrt{s}\, e^{-\sqrt{s}/2\sqrt{\alpha_s/\alpha_1}} ,$$

$$C_3 \frac{K_s}{K_1}\sqrt{\alpha_s/\alpha_1}\left[e^{\sqrt{s}/2} + e^{-\sqrt{s}/2}\right] = C_2 e^{-\sqrt{s}/2\sqrt{\alpha_s/\alpha_1}} . \tag{15}$$

By combining Equations (14) and (15) we obtain the following expression:

$$C_3\left[e^{\sqrt{s}/2} + e^{-\sqrt{s}/2}\right] + \frac{1}{s^2} = -\frac{K_s}{K_1}\sqrt{\alpha_s/\alpha_1}\, C_3\left[e^{\sqrt{s}/2} + e^{-\sqrt{s}/2}\right]$$

or

$$C_3 = -\frac{1}{s^2}\left[\frac{1}{\left[e^{\sqrt{s}/2} + e^{-\sqrt{s}/2}\right] + \beta\left[e^{\sqrt{s}/2} - e^{-\sqrt{s}/2}\right]}\right] \tag{16}$$

where $\beta = \frac{K_s}{K_1}\sqrt{\frac{\alpha_1}{\alpha_s}} = \sqrt{\frac{(K\rho C_p)_s}{(K\rho C_p)_1}}$.

By combining Equations(12) and (16) the following expression is obtained:

$$\tau = \frac{1}{s^2}\left[1 - \frac{e^{\sqrt{s}y'} + e^{-\sqrt{s}y'}}{\left[e^{\sqrt{s}/2} + e^{-\sqrt{s}/2}\right] + \beta\left[e^{\sqrt{s}/2} - e^{-\sqrt{s}/2}\right]}\right]$$

or

$$\tau = \frac{1}{s^2}\left[1 - \frac{e^{\sqrt{s}y'} + e^{-\sqrt{s}y'}}{\left[Ae^{\sqrt{s}/2} - Be^{-\sqrt{s}/2}\right]}\right]$$

where $A = \beta + 1$
$B = \beta - 1.$

By long division

$$\tau = \frac{1}{s^2}\left[1 - \left[\frac{1}{A}e^{\sqrt{s}(y'-1/2)} + \frac{B}{A^2}e^{\sqrt{s}(y'-3/2)} + \frac{B^2}{A^3}e^{\sqrt{s}(y'-5/2)} + \ldots + \frac{1}{A}e^{-\sqrt{s}(y'+1/2)} + \frac{B}{A^2}e^{-\sqrt{s}(y'+3/2)} + \frac{B^2}{A^3}e^{-\sqrt{s}(y'+5/2)} + \ldots\right]\right]$$

or

$$\tau = \frac{1}{s^2} - \frac{1}{A}\frac{1}{s}\left[\frac{e^{-\sqrt{s}(1/2-y')}}{s} + \frac{B}{A}\frac{e^{-\sqrt{s}(3/2-y')}}{s} + \left[\frac{B}{A}\right]^2\frac{e^{-\sqrt{s}(5/2-y')}}{s} + \ldots + \frac{e^{-\sqrt{s}(1/2+y')}}{s} + \frac{B}{A}\frac{e^{-\sqrt{s}(3/2+y')}}{s} + \left[\frac{B}{A}\right]^2\frac{e^{-\sqrt{s}(5/2-y')}}{s} + \ldots\right].$$

E. Time Domain Solution

The inverse transform for the solid is:

$$T' = t' - \frac{1}{A}\int_0^{t'} \left[\operatorname{erfc}\left[\frac{1/2 - y'}{2\sqrt{\theta}}\right] + \frac{B}{A}\operatorname{erfc}\frac{3/2 - y'}{2\sqrt{\theta}} \right.$$

$$+ \left[\frac{B}{A}\right]^2 \operatorname{erfc}\left[\frac{5}{2} - y'\right] + \ldots + \operatorname{erfc}\left[\frac{1/2 + y'}{2\sqrt{\theta}}\right]$$

$$\left. + \frac{B}{A}\operatorname{erfc}\left[\frac{3/2 + y'}{2\sqrt{\theta}}\right] + \left[\frac{B}{A}\right]^2 \operatorname{erfc}\left[\frac{5/2 + y'}{2\sqrt{\theta}}\right] + \ldots \right] d\theta$$

or

$$T' = t' - \frac{1}{A}\sum_{n=0}^{\infty}\left[\frac{B}{A}\right]^n \int_0^{t'} \left[\operatorname{erfc}\left[\frac{2n + 1 - y'}{2\sqrt{\theta}}\right] \right.$$

$$\left. + \operatorname{erfc}\left[\frac{2n + 1 + y'}{2\sqrt{\theta}}\right]\right] d\theta\,, \quad -1/2 < y' < 1/2\,. \tag{17}$$

U.S. GOVERNMENT PRINTING OFFICE /50-113